Polarization of Λ - hyperons in Au-Au collisions at NICA energies

A.V. Zinchenko[a], O.V. Teryaev[b], M.I. Baznat[b,c]

[a] P. G. Demidov Yaroslavl State University, Yaroslavl, Russia
[b] Joint Institute for Nuclear Research, Dubna, Russia
[c] Institute of Applied Physics, Chisinau, Moldova

International Conference on Quantum Filed Theory, High-Energy Physics, and Cosmology, Dubna, Russia, 21 July 2022

Outline

Introduction

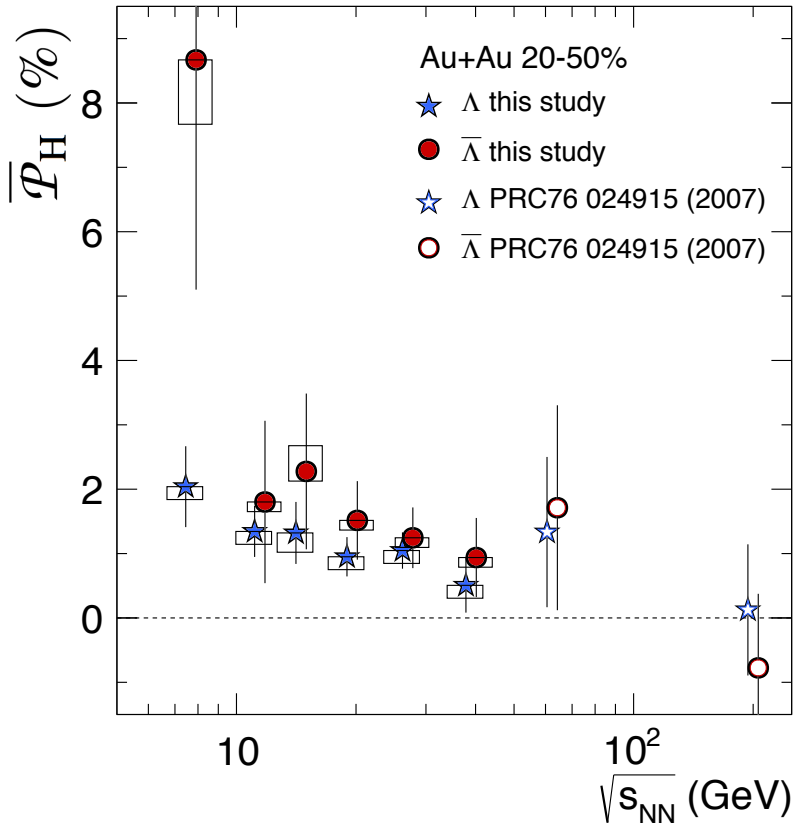

fig: 1. The average polarization $\overline{\mathcal{P}}_{\mathrm{H}}$, where $\mathrm{H} = \Lambda$ or $\bar{\Lambda}$, from 20-50% central Au+Au collisions is plotted as a function of the collision energy $\sqrt{s_{NN}}$ (STAR data [Nature 548 (2017) 62-65])

PHSD model

- The Parton-Hadron-String Dynamics (PHSD) (W. Cassing, E. L. Bratkovskaya, Phys. Rev. C78 (2008) 034919, arXiv:0808.0022 [hep-ph]) is the microscopic off-shell transport approach that consistently describes the full evolution of a relativistic heavy-ion collision from the initial hard scatterings and string formation through the dynamical deconfinement phase transition to the quark-gluon plasma as well as hadronization and to the subsequent interactions in the hadronic phase
- To calculate the vorticity field, the velocity field $\vec{v}(x)$ needs to be known. In relativistic system, its definition is not unique. Several types of velocity field, $\vec{v}_1$, $\vec{v}_2$, and $\vec{v}_3$, are introduced:

$$v_1^a(x) = \frac{\sum_i p_i^a \, F(x, x_i)}{\sum_i p_i^0 \, F(x, x_i)},$$

$$v_2^a(x) = \frac{1}{\sum_i F(x, x_i)} \sum_i \frac{p_i^a}{p_i^0} \, F(x, x_i),$$

$$v_3^a(x) = \frac{\sum_i p_i^a \, F(x, x_i)}{\sum_i [p_i^0 + (p_i^a)^2 / p_i^0] \, F(x, x_i)},$$

  where $a = 1, 2, 3$ are the spatial indices, p_i^a and p_i^0 are the momentum and energy of the i-th particle, and the summation is over all the particles.
- The first definition, $\vec{v}_1$, is used in the following.

Vorticity structure

- Similar to the velocity, several definitions of the vorticity exist
- Non-relativistic and relativistic kinetic vorticities:

$$\varpi_{\mu\nu} = \frac{1}{2}(\partial_\nu v_\mu - \partial_\mu v_\nu)\,, \quad \omega_{\mu\nu} = \frac{1}{2}(\partial_\nu u_\mu - \partial_\mu u_\nu)\,,$$

where u_ν is a four-vector of the relativistic velocity field:

$$u^\nu(t,\vec{x}) = \gamma(t,\vec{x})\,(1,\,\vec{v}(t,\vec{x}))\,, \quad \gamma(t,\vec{x}) = \frac{1}{\sqrt{1-\vec{v}^{\,2}(t,\vec{x})}}$$

- In the case of the relativistic vorticity, γ-factor has a significant influence on the fireball boundaries, strengthening vorticity value as shown in Fig. 2

Vorticity structure

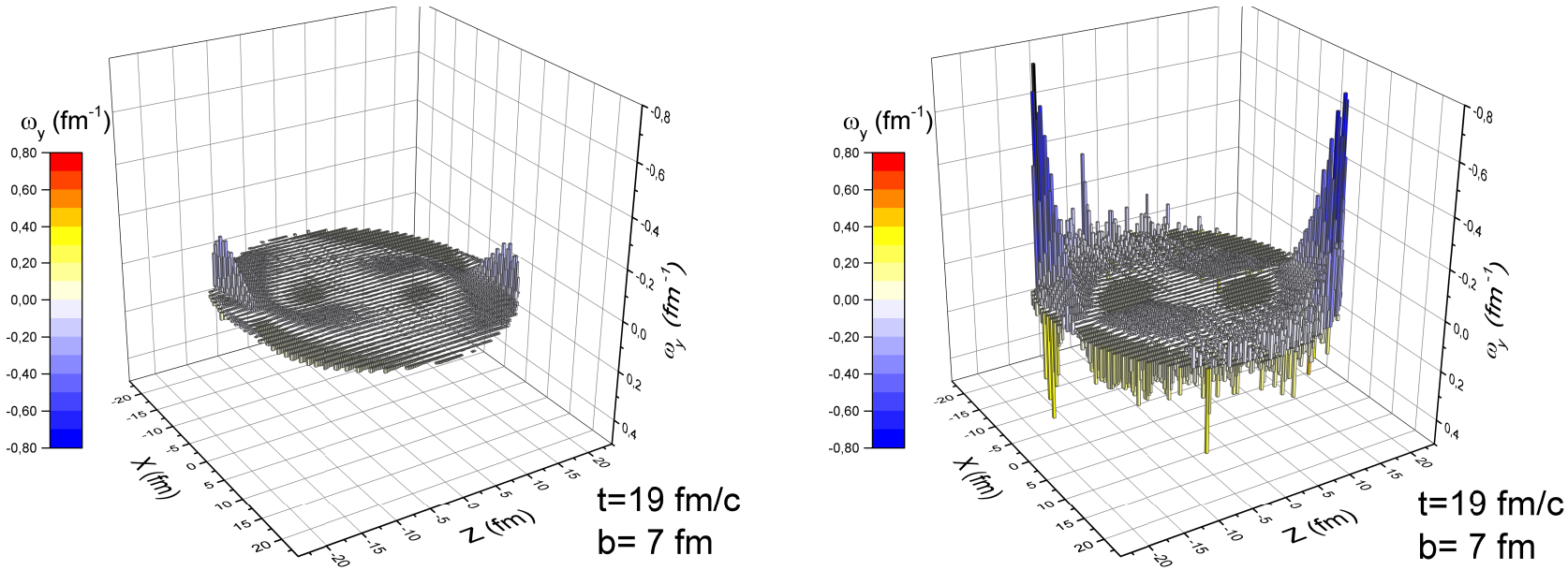

fig: 2. Y-projection of the vorticity $\vec{\omega}$ in the reaction plane xz $(y = 0)$ in the case of the non-relativistic (left plot a) and relativistic (right plot b) definitions at the energy $\sqrt{s} = 7.7$ GeV

It takes the largest value on the boundaries of the fireball and spectators, and it has the same sign on both boundaries, which together gives a non-zero ω_y vorticity

Vorticity structure

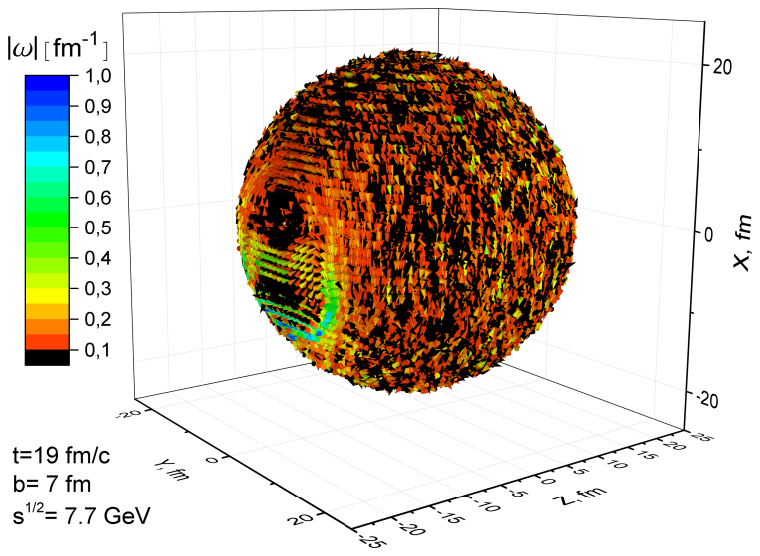

(a)

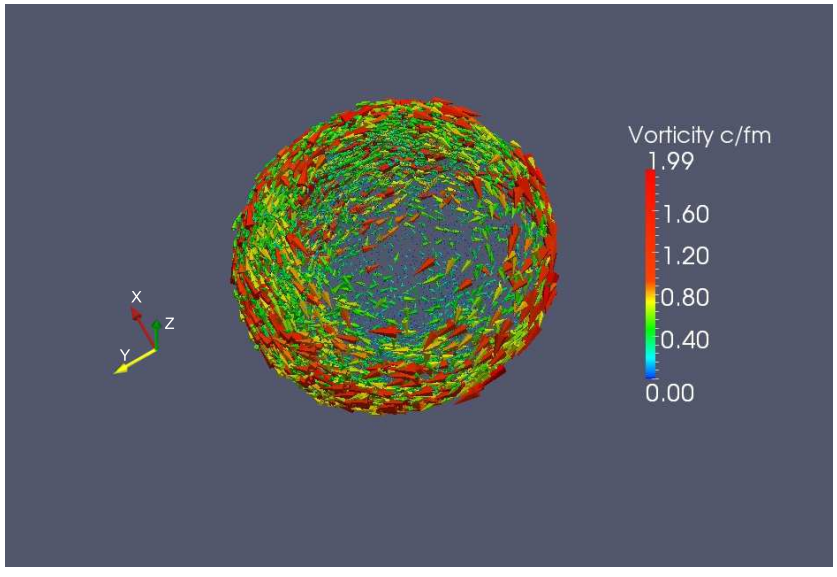

(b)

fig: 3. Vortex sheet in the PHSD (plot a) and QGSM (plot b) models

Since 15 fm/c the so-called vortex sheet begins to form on the boundary of the fireball at the energy $\sqrt{s} = 7.7$ GeV. It is observed both in the Quark-Gluon String Model (QGSM) and PHSD model. In the PHSD model, the structure has a significant vorticity on the border of participants and spectators as shown in Figs. 2b and 3

Vorticity structure

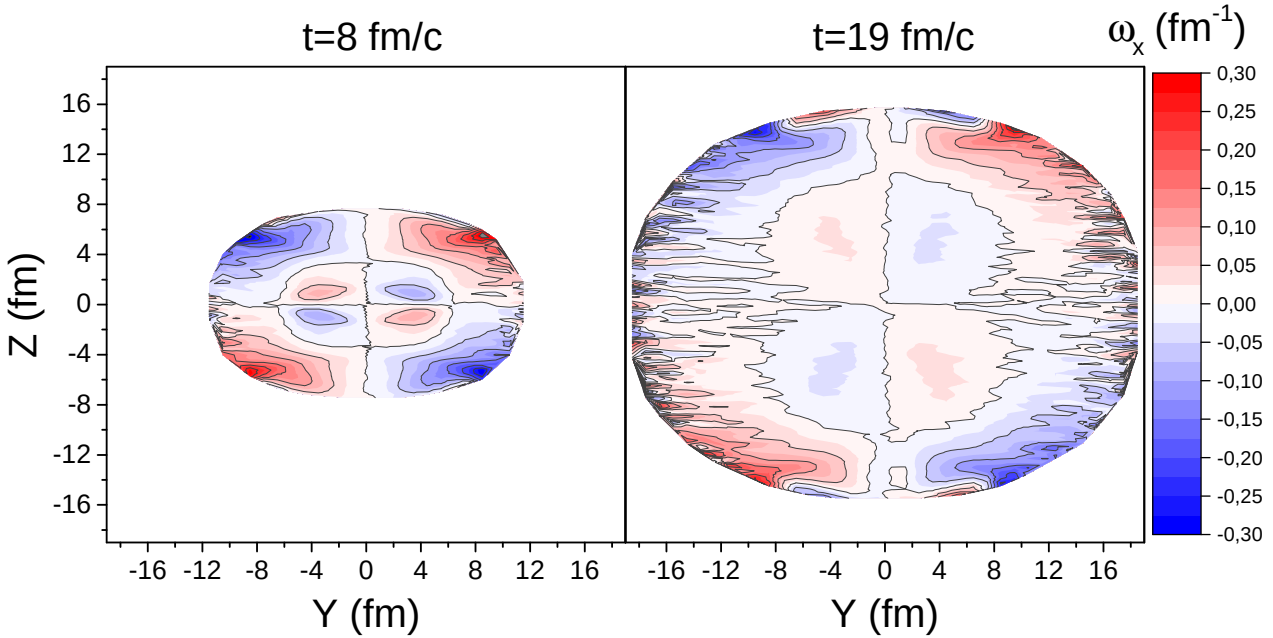

fig: 4. Quadrupole structure of relativistic vorticity ω_x in Au+Au at $\sqrt{s} = 7.7$ GeV, $x = 0$, impact parameter $b = 7$ fm

The presence of a vortex sheet in the perpendicular plane zy is seen. An increase in the x-projection of vorticity is observed around the boundary of the fireball and there are maximums at the boundary with spectators, as in plane xz. In addition, a mirror quadrupole structure with an internal part having an opposite sign with respect to the corresponding external region is also seen

Vorticity structure

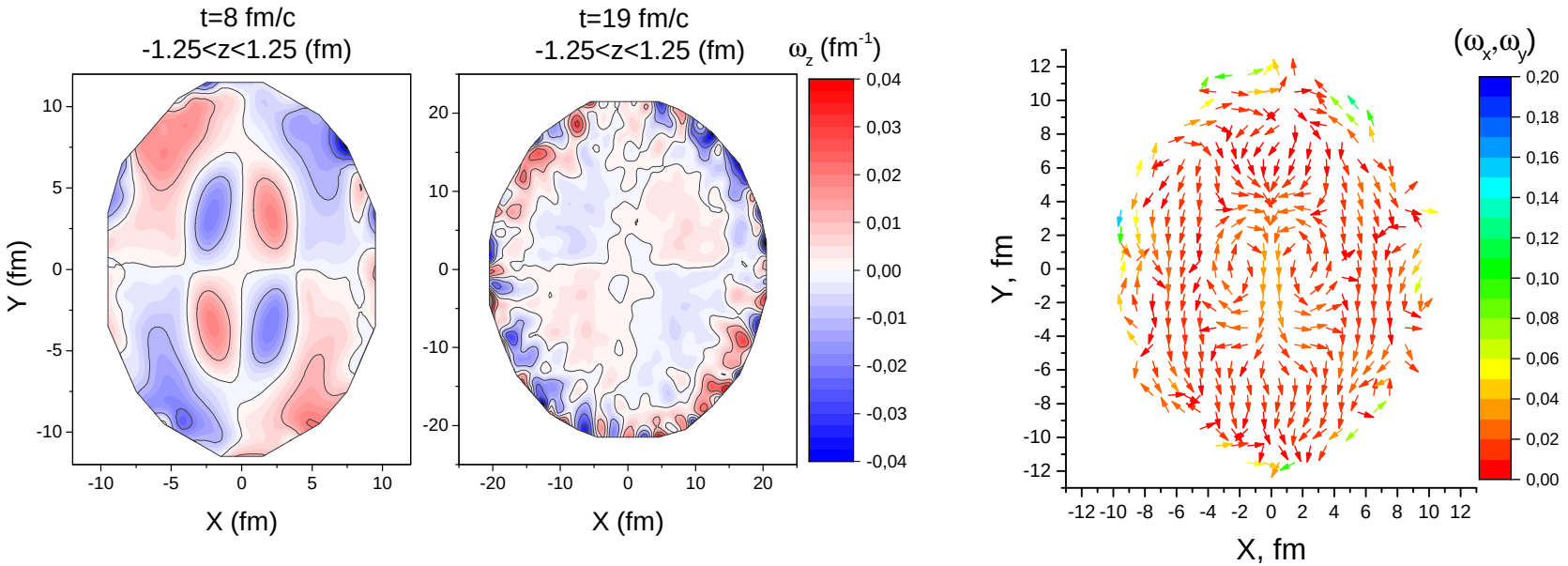

fig: 5. (a) Quadrupole structure of relativistic vorticity ω_z in Au+Au at $\sqrt{s} = 7.7$ GeV at times $t = 8$ fm/c and $t = 19$ fm/c. Averaging is performed over the 2.5 fm range in the $Z = 0$ layer. (b) The structure of the transverse vorticity $\vec{\omega}_\perp = (\omega_x, \omega_y)$ in Au+Au for $b = 7$ fm in the center of the fireball, $Z = 0$, at the same energy at $t = 8$ fm/c

Vorticity structure

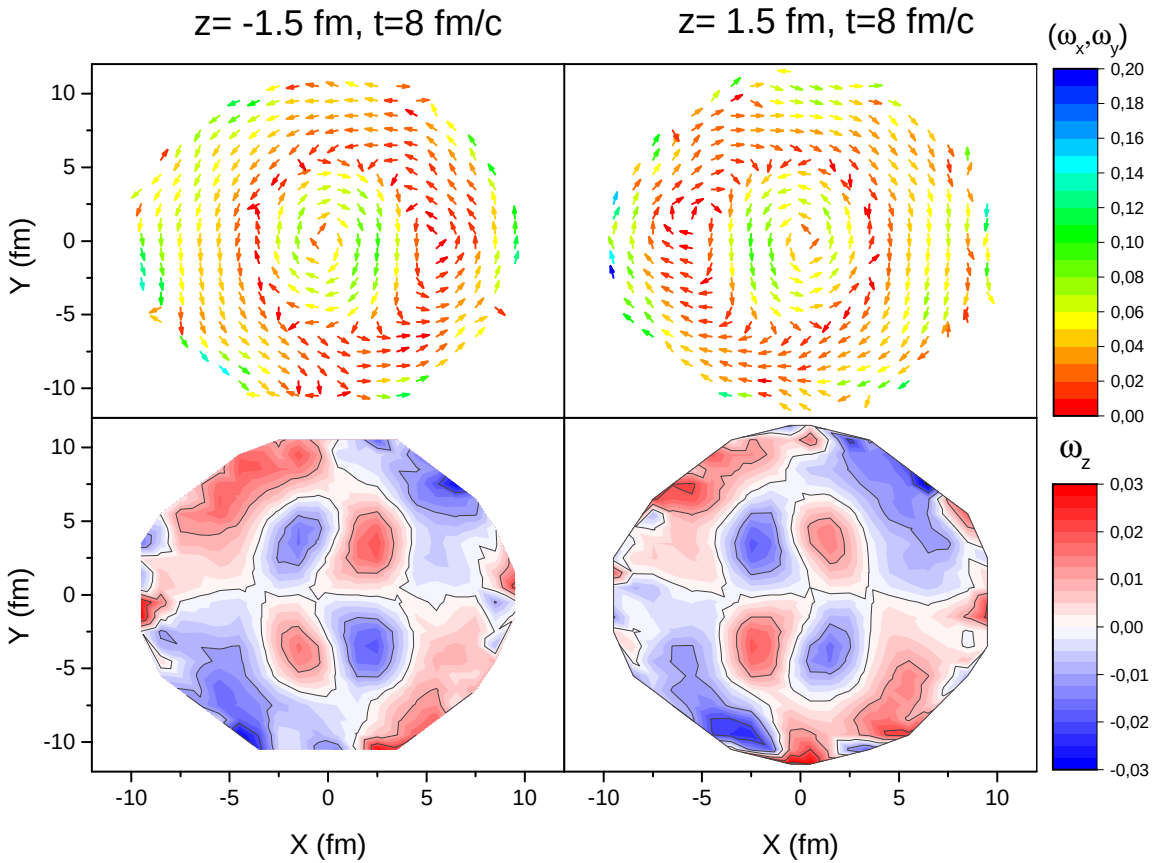

fig: 6. The quadrupole structure of relativistic vorticity ω_z in Au+Au at $\sqrt{s} = 7.7$ GeV (bottom line) and corresponding structure of the transverse vorticity $\vec{\omega}_\perp$ (top line) in the same Z-layer at the same time.

Vorticity structure

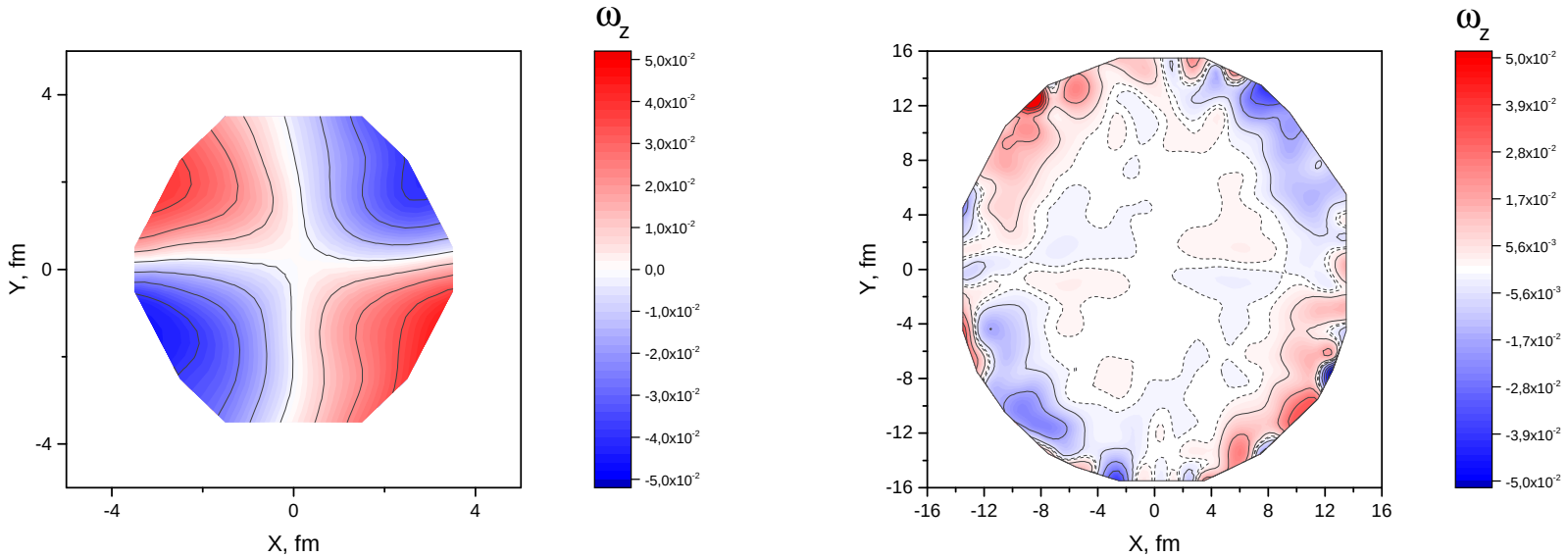

(a) (b)

fig: 7. The quadrupole structure of the relativistic vorticity ω_z in Au+Au collisions for $b = 8$ fm at $\sqrt{s} = 7.7$ GeV at times $t = 9.5$ fm/c (left plot) and $t = 13$ fm/c (right plot) without $P - P$ potential. Averaging is performed over the 5 fm range in the $Z = 0$ layer.

Vorticity structure

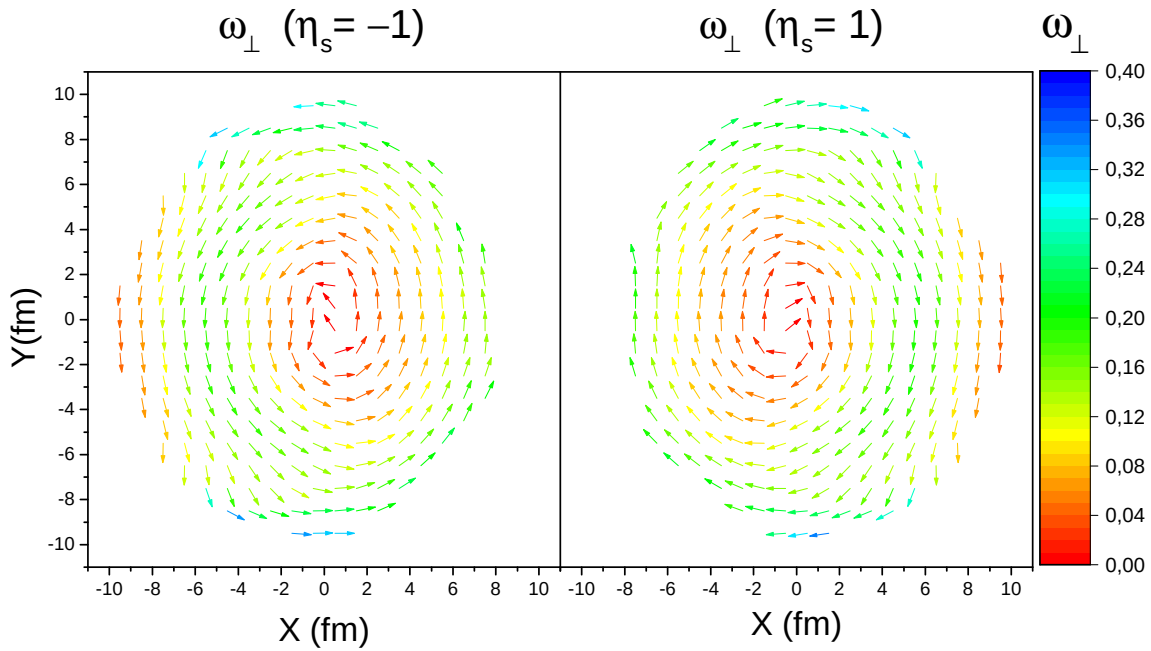

fig: 8. The distribution of the transverse vorticity $\vec{\omega}_\perp = (\omega_x, \omega_y)$ in the transverse plane at the longitudinal positions $\eta_s = -1$ (left plot) and $\eta_s = 1$ (right plot), where $\eta_s = (1/2)\ \ln\left[(t+z)\,/\,(t-z)\right]$, for $b = 5$ fm at $\sqrt{s} = 7.7$ GeV and $t = 9.5$ fm/c. It is consistent with existing results (arXiv:1810.00151 [nucl-th]), where similar structures for the thermal vorticity are obtained.

Vorticity structure

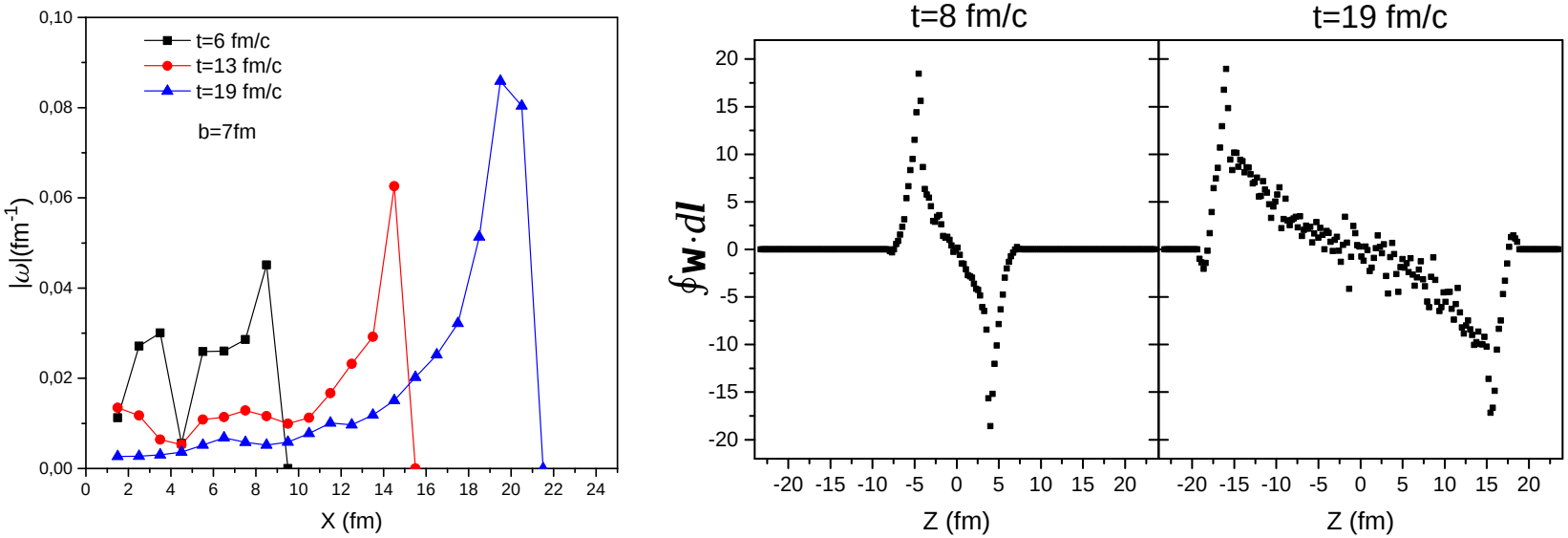

(a) (b)

fig: 9. (a) The dependence of the vorticity modulus on the fireball radius for $b = 7$ fm in $Z = 0$ plane at $\sqrt{s} = 7.7$ GeV at different times. (b) Vorticity field circulation in the XY plane as a function of Z at $t = 8$ fm/c and $t = 13$ fm/c.

From the analysis presented, we conclude that the vorticity field has a spherical elongated shape at poles of which (along Z-axis) it is maximum and half of this sphere rotates in different directions, having the opposite rotation in the center. The total rotation tends to zero when approaching $Z = 0$. We can see this by taking the circulation of the vorticity vector at various points Z in XY-plane (Fig. 8b). At the same time, the vorticity modulus at $Z = 0$ grows towards the boundary (except at times of order 6 fm/c, when there is a significant vorticity modulus inside the fireball) of the fireball and increases with time. This means that near $Z = 0$ a distinguished direction of the vorticity field rotation is absent and, when moving away from zero, two opposite rotations are formed.

"Hubble low" in PHSD

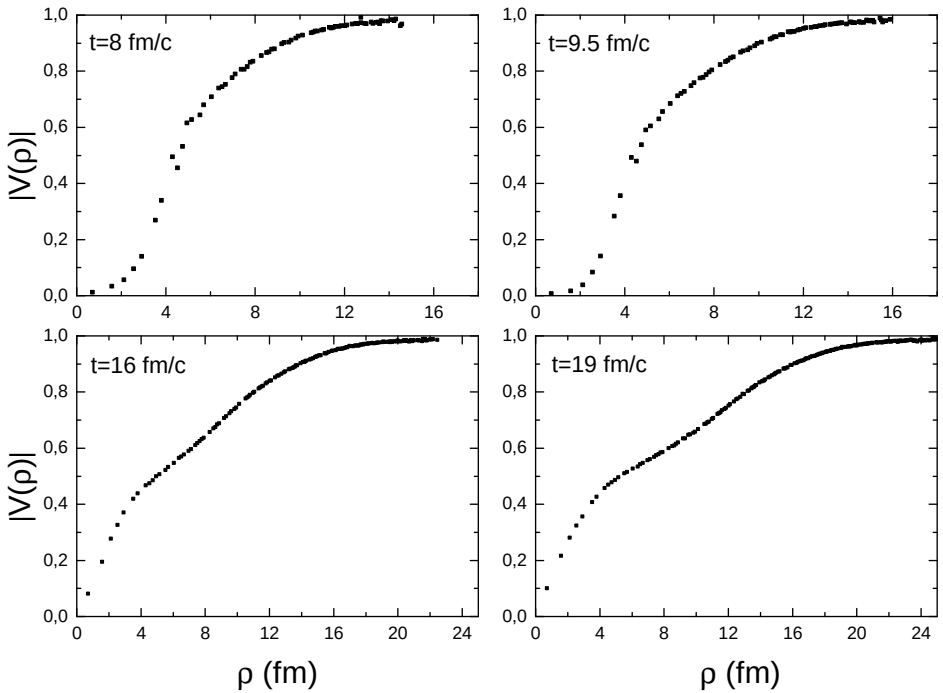

fig: 10. The dependence of particles' velocity on the transverse radius $\rho = \sqrt{x^2 + y^2}$ in $z = 0$ plane with $b = 7$ fm at $\sqrt{s} = 7.7$ GeV.

The dependence of particles' velocity in the fireball at different times is seen. There is an area with a linear dependence of the velocity at freeze out time.

"Hubble low" in PHSD

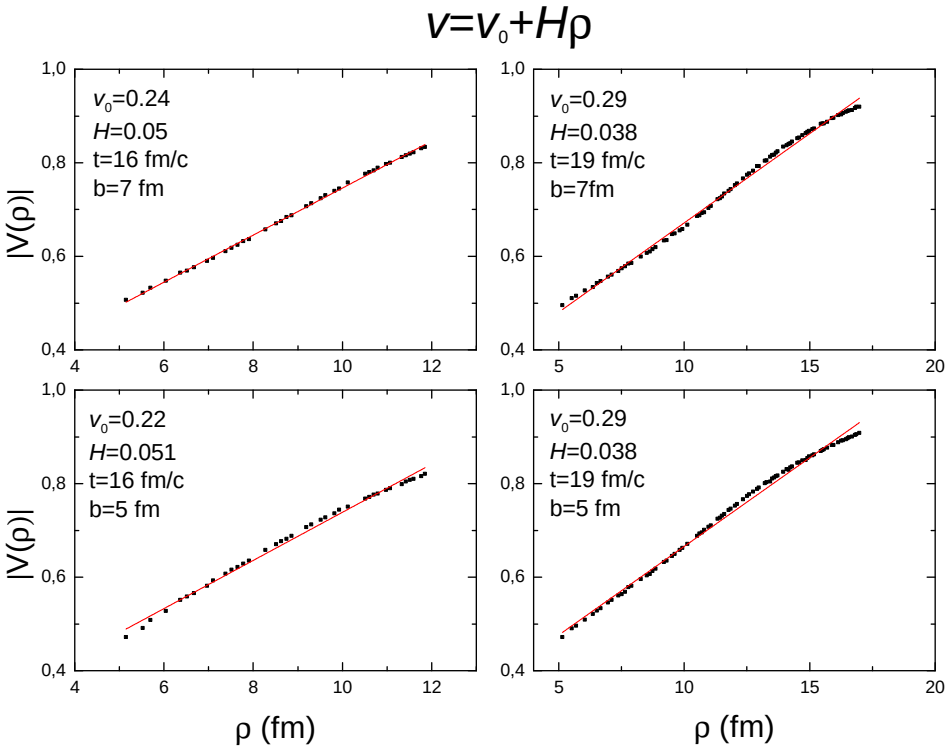

fig: 11. Dependence of particles' velocity on the transverse radius $\rho = \sqrt{x^2 + y^2}$ in $z = 0$ plane as the "Hubble law" with $b = 5$ fm and $b = 7$ fm at $\sqrt{s} = 7.7$ GeV.

A linear dependence of the velocity in the medium area of the fireball at times exceeding 15 fm/c is seen. This area can be called the "Little Bang" and the "Hubble law" with a constant H can be defined.

"Hubble low" in PHSD

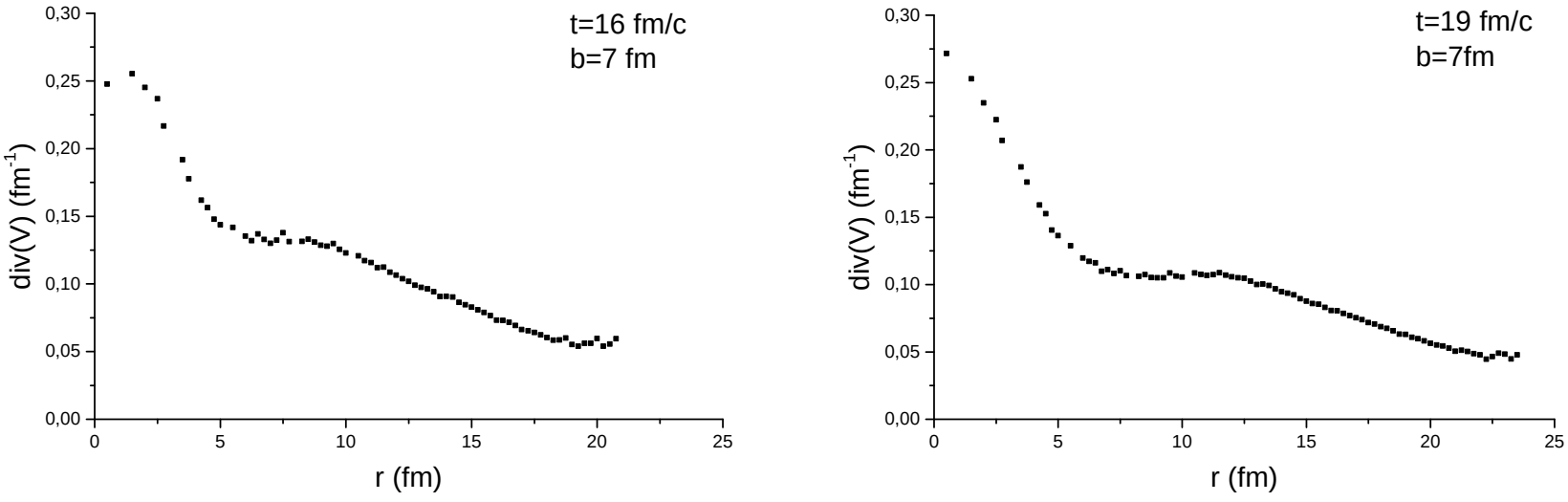

fig: 12. The dependence of the particle velocity divergence on the distance to the fireball.

Only in a small area, where particles are already form and fly apart without interaction, the divergence has the form $\mathrm{div}\,(\vec{v}) = \mathrm{const}$. It is possible to determine a uniform expansion for $6 < \rho < 9$ fm at $t = 16$ fm/c and $6.5 < \rho < 11.5$ fm at $t = 19$ fm/c. This region corresponds to a half of the linear velocity region. It determines a constant value of the divergence $\mathrm{div}\,(\vec{v}) = 0.14$ fm^{-1} at $t = 16$ fm/c and $\mathrm{div}\,(\vec{v}) = 0.11$ fm^{-1} at $t = 19$ fm/c, which results into $\mathrm{div}\,(\vec{v}) \simeq 3\,H$.

Helicity separation

Helicity contributes directly to the polarization of hyperons

$$< \Pi_0^\Lambda > = < \frac{m_\Lambda}{N_\Lambda\, p_y} > \frac{N_c}{2\pi^2} \int d^3x\, \mu_s^2(x) \gamma^2 \epsilon^{ijk} v_i \partial_j v_k,$$

in the so-called axial vortical effect approach. The effect is proportional to vorticity and helicity of the strong interacting medium, and, in particular, to helicity separation effect discovered in the kinetic QGSM by M. Baznat et al. (Phys. Rev. C88 (2013) 061901; arXiv:1301.7003 [nucl-th]). The hydrodynamic helicity is contained within the integral $H \equiv \int d^3x\, (\vec{v} \cdot \vec{\omega})$. Helicity separation effect receives the significant contribution $\sim v_y \omega_y$ from the transverse components of velocity and vorticity. It is easily explained by the same signs of transverse vorticities in the "upper" and "lower" (w.r.t. reaction plane) half-spaces, combined with the opposite signs of velocities. Even larger contribution of longitudinal components of velocity and vorticity, $\sim v_z \omega_z$, implies the appearance of the "quadrupole" structure of longitudinal vorticity.

Helicity separation

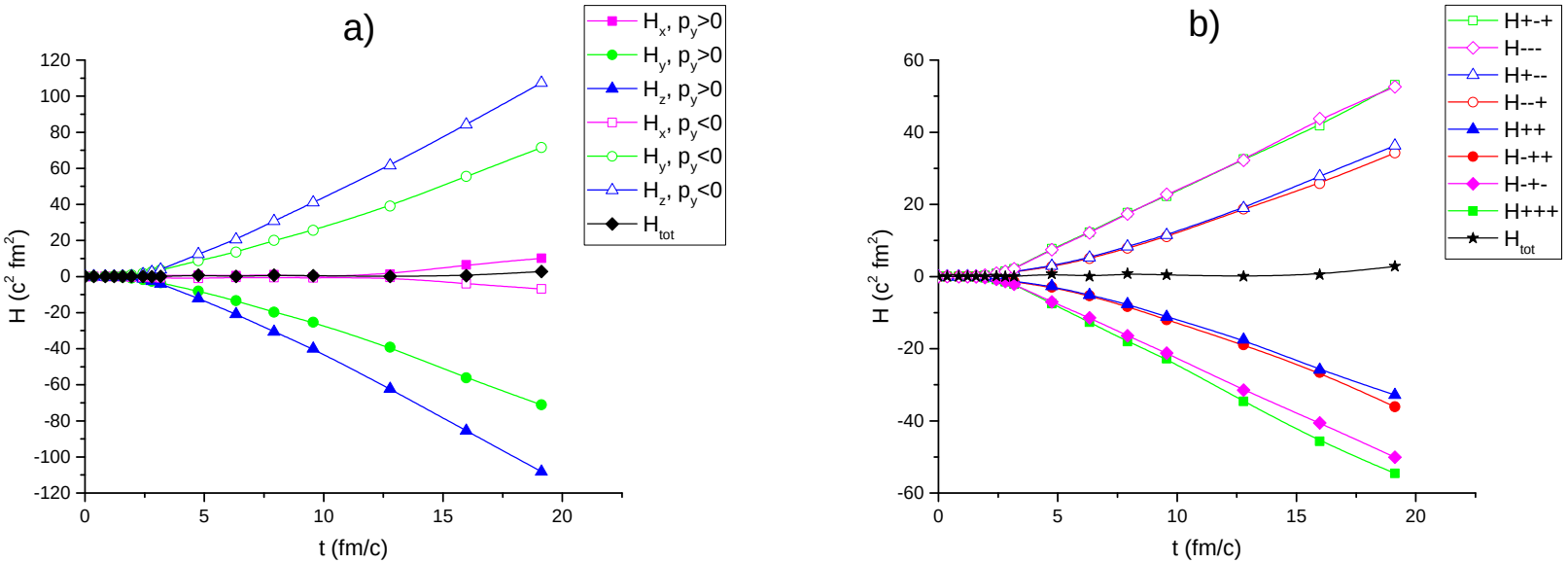

fig: 13. a) Helicity H (fm^2c^2) separation relative to the y-component of the momentum for the impact parameter $b = 7$ fm at $\sqrt{s} = 7.7$ GeV. b) Helicity separation relative to spatial octants for the same impact parameter at the same energy. "+++" means that the integration is performed in the octant $x > 0$, $y > 0$, $z > 0$, "$-\,-\,-$" is in the opposite octant $x < 0$, $y < 0$, $z < 0$ and etc..

Polarization of Λ-Hyperons

The polarization of Λ-hyperons is calculated within the approach exploring local equilibrium thermodynamics (F. Becattini et al., Eur. Phys. J. C75 (2015) 191; arXiv:1403.6265 [hep-th]) and in the axial vortical effect approach with centrality $20-50\,\%$, energy $\sqrt{s}=7.7$ GeV and rapidity $|y|<1$, where $y=(1/2)\ln((E+p_z)/(E-p_z))$. In thermodynamic approach, the spin vector $\vec{S}^*$ averaged over the $\vec{p}_\Lambda$ direction is determined by

$$\langle \vec{S}^*_\Lambda \rangle_{\vec{n}_p} = \frac{(1-n_\Lambda)}{4M_\Lambda}\left(E_\Lambda + \frac{1}{3}\frac{\vec{p}^{\,2}_\Lambda}{E_\Lambda + m_\Lambda}\right) \mathrm{rot}\vec{\beta}\,.$$

where $\vec{\beta}=\vec{v}/T$ is thermodynamical velocity. The results for $\Pi_0^\Lambda = 2\langle S^*_{\Lambda y}\rangle_{\vec{n}_p}$ are $\Pi_0^\Lambda = 0.7\%$ for thermodynamic approach and $\Pi_0^\Lambda = 8\%$ for anomaly one, of which the last is very sensitive to chemical potential. The order of magnitude difference can be related firstly in the choice of velocity definition and secondly in the sensitivity to thermodynamic quantities.

Summary

1. Simulations of Au+Au collisions in the PHSD model are performed. The vorticity field structure in collisional medium is studied.
2. The "Little Bang" structure of the velocity field is found.
3. The helicity separation effect is discovered in the PHSD model.
4. The values of Λ-hyperons polarization in the termodynamical and axial-vortical-effect approaches are calculated.